Secondary-Sphere Preorganization Enables Nickel-Catalyzed Nitrile Hydroboration

Journal:	*ChemComm*
Manuscript ID	CC-COM-08-2023-004229.R2
Article Type:	Communication

COMMUNICATION

Secondary-Sphere Preorganization Enables Nickel-Catalyzed Nitrile Hydroboration

Received 00th January 20xx,
Accepted 00th January 20xx

DOI: 10.1039/x0xx00000x

Medina Afandiyeva,† [a] Xijue Wu, † [a] William W. Brennessel,[a] Abhishek A. Kadam,[a] and C. Rose Kennedy* [a]

Herein, we describe nickel-catalyzed nitrile hydroboration with pinacolborane, wherein a tethered NHC-pyridonate ligand enables efficient catalysis (5 mol% [Ni], ≤6 h reaction time) at room temperature. Mechanistic studies, including isolation of the catalytically relevant intermediates, shed light on the cooperative role of the ligand in activating both reagents simultaneously.

Primary alkyl amines are prevalent among agrochemicals, pharmaceuticals, polymers, and pigments (Scheme 1A).[1, 2] Compared to direct ammonia alkylation, which typically results in competitive over-alkylation, synthetic strategies involving reduction of unsaturated, N-containing groups provide efficient access to primary alkyl amines from feedstock reagents.[1, 3] Nitriles are particularly attractive synthons for this route due to the ease of CN incorporation through direct cyanation and substitution techniques.[4] For example, adiponitrile is produced on million-ton scale by nickel-catalyzed hydrocyanation of butadiene for industrial production of nylon 66.[5] However, the strong C≡N bond (BDE = 750.0 kJ/mol)[6] often necessitates forcing reduction conditions (high temperature, high H_2 pressure, and long reaction time) or use of superstoichiometric metal hydride reductants, which limit utility beyond all-hydrocarbon substrates.[7-9]

Catalytic nitrile hydroboration with a weakly nucleophilic monohydride borane, followed by hydrolysis of the resulting diborylamine, constitutes an attractive alternative to the forcing conditions above.[10] Nitrile hydroboration also serves as an informative testing ground for metal–ligand-cooperative catalysis due to the involvement of both Lewis basic (nitrile) and acidic (borane) substrates.[11] As such, both main-group[6, 12-15] and transition metal catalysts [10, 16-25] have been developed previously for nitrile hydroboration. However, the breadth of compatible substrates, requisite reaction temperatures, and levels of mechanistic insight have varied substantially among these examples, with opportunities for improvement across the board (Scheme 1B).

We recently reported the synthesis and characterization of a family of anionic nickel complexes supported by bidentate NHC-pyridonate ligands.[26] This work provided evidence for direct pyridonate oxygen involvement in highly regioselective

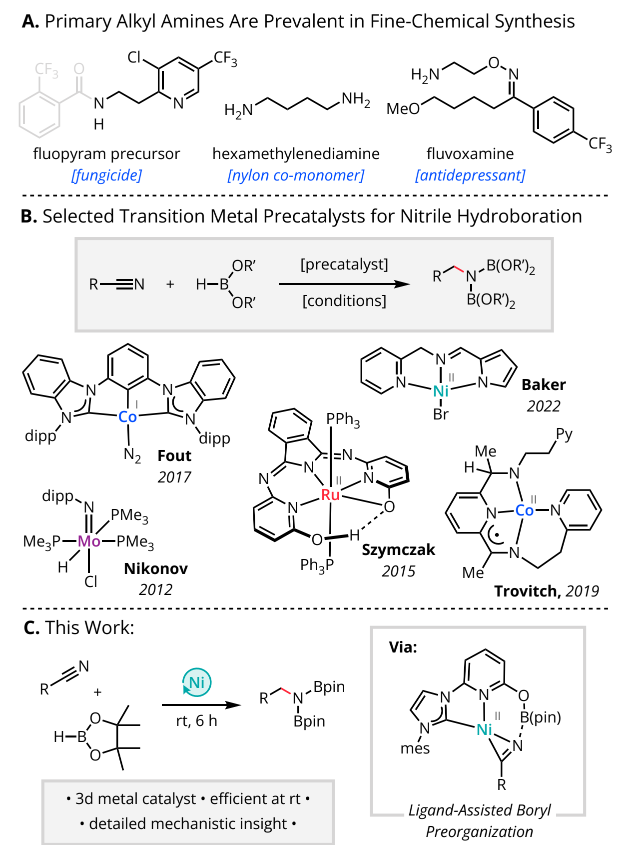

Scheme 1. State-of-the-Art in Nitrile Hydroboration for Access to Alkyl Amines.

[a.] *Department of Chemistry, University of Rochester, Rochester, NY 14627, USA*
† Authors M. A. and X. W. contributed equally; both are entitled to list their own name first on publication lists.
Electronic Supplementary Information (ESI) available: [details of any supplementary information available should be included here]. See DOI: 10.1039/x0xx00000x

(>99:1 r.r.) catalytic hydroboration of styrene with HBpin. Based on the observation that the nickel precatalysts also underwent facile η^2-coordination of acetonitrile, we hypothesized that they would similarly catalyze reactions with more polar nitrile substrates. Herein, we report that the NHC-pyridonate-supported Ni(0) complex [K(18-crown-6)][(**L1**)Ni(cod)] (**L1** = 1-(2,4,6-trimethylphenyl)-3-(6-oxidopyridin-2-yl)-imidazol-2-ylidene) catalyzes double hydroboration of nitriles to primary alkyl amines (Scheme 1C). Although Szymczak and co-workers previously described nitrile and ketone hydroborations using a ruthenium catalyst supported by a conceptually similar pyridone-containing pincer ligand (Scheme 1B),[17] our report complements this prior work by demonstrating mechanistically distinct ligand-assisted nucleophile and electrophile delivery to the substrate, enabled by a terrestrially abundant 3d metal. Our work thus provides a blueprint for catalytic method development leveraging ligand assistance with both hydrocarbyl and polar substrates.

We initiated our studies using benzonitrile **1a** as a model substrate in the presence of excess HBpin (4 equiv) and 5 mol% [K(18-crown-6)][(**L1**)Ni(cod)] in toluene. These conditions afforded double hydroboration product **2a** (87%, no other products observed) within 6 hours at room temperature (approx. 22 °C). Using ligands **L2** or **L3** instead of **L1** resulted in decreased product yield (Scheme 2, entries 1–3). Decreasing the catalyst loading to 2.5 mol% slowed conversion, requiring extended reaction times. However, running the reaction under solvent-free conditions improved the efficiency at this lower catalyst loading (entries 4–5). Entries with lower equivalents of HBpin required longer reaction times but proceeded cleanly (entry 6). Generating the precatalyst in situ by mixing [Ni(cod)$_2$], **L1**•HCl, KO^{t}Bu, and 18-crown-6 prior to substrate addition resulted in selective **2a** formation with a yield comparable to that obtained with the single-component precatalyst (entry 7). Control experiments using ligands with an isomeric 4-pyridone motif (**L4**) or pyridine in place of pyridone (**L5**) delivered product in substantially decreased yields, even after extended reaction times (Scheme 2, entries 8–9). These findings suggest a critical role for the 2-pyridonate oxygen beyond an inductive effect. No product was observed without ligand indicating that [Ni(cod)$_2$] alone could not act as an efficient pre-catalyst (entry 10). Additional control experiments using only [K(18-crown-6)][**L1**] or [K(18-crown-6)][**L6**] without [Ni] showed no product formation (entry 11), indicating that the pyridonate motif alone was not inducing “hidden boron catalysis”.[27] This conclusion was reinforced by the observation that *N,N,N′,N′*-tetramethylethylene diamine (TMEDA), which would sequester any BH_3 generated in situ, did not inhibit reactivity (see ESI).[27]

Nitrile-containing substrates with varied electronic and steric properties were evaluated under the optimized conditions (Scheme 3). Aryl nitriles bearing electron-neutral (**1b–c**), electron-donating (**1d**), and electron-withdrawing (**1e–h**) substituents reacted readily to afford the corresponding benzylamines in 32–72% isolated yield upon hydrolysis. *Ortho-* (**1c**) and *meta-* (**1f**) substituents did not interfere with productive reaction. Boronic ester (**1g**) and bulky carboxamide (**1h**) groups were compatible with the reaction conditions and

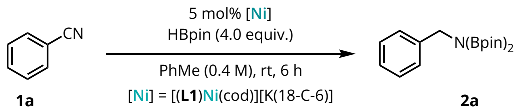

entry	deviation from standard conditions	yield of **2a**
1	none	87%
2	**L2** instead of **L1**	46%
3	**L3** instead of **L1**	81%
4[a]	2.5 mol% [Ni]	56%
5	2.5 mol% [Ni], no solvent	88%
6	3 equiv. HBpin, 16 h	81%
7[b]	**L1**•HCl + KO^{t}Bu + Ni(cod)$_2$ as [Ni]	85%
8[b]	**L4**•HCl + KO^{t}Bu + Ni(cod)$_2$ as [Ni]	34%
9	[(**L5**)Ni(cod)] as [Ni]	29%
10	[Ni(cod)$_2$] as [Ni],no ligand	n.d.[d]
11	[K(18-crown-6)][**L1** or **L6**], no [Ni]	n.d.[d]
12[a,c]	no [Ni], no ligand	n.d.[d]

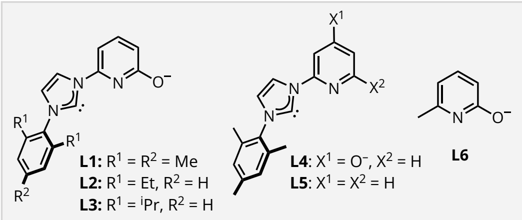

Scheme 2. Optimization of reaction conditions. Reactions were conducted in duplicate using benzonitrile **1a** (0.2 mmol, 1.0 equiv) and HBpin (0.8 mmol, 4.0 equiv) at ambient temperature (~22 °C) in a N_2 atmosphere glovebox. Yields were determined from the relative ^{1}H NMR integrations of **2a** vs. 1,3,5-trimethoxybenzene (0.1 mmol) added after the reaction as the internal standard. ^{a} 24 h reaction time. ^{b} Ligand generated in situ by premixing **L**•HCl (10 mol%), KO^{t}Bu (20 mol%), and 18-crown-6 (10 mol%) prior to the addition of other reagents. ^{c} benzene-d_6 used as a solvent. ^{d} n.d.: not detected = <2%.

allowed for chemoselective nitrile hydroboration without any apparent catalyst inhibition through competitive binding of the *p*-substituents. However, ketone- (**1q**) and ester-containing (**1r**) substrates underwent exhaustive hydroboration to afford the corresponding amino alcohol products (**3q, r**). Halogens (X=Cl or Br) were not compatible with the catalytic conditions and resulted in ~5% yield of the protodehalogenated product with concomitant catalyst death. We hypothesize that oxidative addition of the nickel precatalyst into the C–X bond is competitive with hydroboration in these cases. Nonetheless, the catalytic conditions are suitable for hydroboration of unactivated alkyl nitrile substrates (**2l–p**). Even for substrates featuring nitrile and aryl groups separated by an alkyl linker (**2n, o**), no products derived from competitive chain-walking were detected. Adiponitrile (**1p**) underwent hydroboration at both nitrile sites to yield tetraboryl hexamethylenediamine (**2p**) en route to **3p**, which is a monomer for nylon 66 production.

To better understand the mechanistic basis for the observed reactivity patterns, we initiated a series of stoichiometric studies with the aim of characterizing catalytically relevant intermediates. We observed previously that in the presence of acetonitrile, [K(18-crown-6)][(**L1**)Ni(cod)] underwent ligand exchange with MeCN to form an η^2-coordinated, 16-electron complex with secondary interactions between the acetonitrile N and [K(18-crown-6)]$^+$ countercation.[26] Treating [K(18-crown-6)][(**L1**)Ni(cod)] with nitriles **1a**, **1k** or **1m** (1.0 equiv.) similarly afforded the corresponding η²-nitrile adduct **5a–c** (see Supporting Information). All three complexes were characterized by NMR and single crystal X-ray diffraction (SC–XRD) and exhibited structural characteristics similar to the MeCN complex described previously.[26] Although these complexes did not undergo any perceptible change when treated with *1 equiv*. of HBpin in stoichiometric experiments, neither **5b** nor **5c** were detected under catalytic conditions involving a *large excess* of HBpin relative to [Ni]. However, the identities of the true catalyst resting states could not be deduced readily through NMR analysis alone.

Serendipitously, we isolated *N,N*-diboryliminium complex **6** from a catalytic reaction with substrate **1m** (Scheme 4A). SC-XRD revealed the molecular structure featuring η²-coordination of N,N-diboryliminium ion along with a secondary Lewis acid-base interaction between one boryl group on nitrogen and the pyridonate O. To better understand the relevance of this adduct as an on- or off-cycle intermediate, we devised a fluorine-tagged substrate model (*Z*)-1-(4-fluorophenyl)-*N*-phenylmethanimine (**7**). Treating [K(18-crown-6)][(**L1**)Ni(cod)] with **7** (1.0 equiv.) yielded [Ni]-imine complex **8** (Scheme 4B). Exposing **8** to HBpin (1.0 equiv) resulted in little perceptible change in the composition of [Ni]; however, hydroborated product **9** grew in over the course of many hours (5% yield after 24 hours). In contrast to the nitrile-bound system, imine adduct **8** *was* observed as the primary catalyst resting state under catalytic conditions with excess HBpin. Although these experiments cannot provide conclusive evidence, they are consistent with on-cycle involvement of imine complexes resembling **6** and **8** (Scheme 4).

On the basis of these experimental observations, we propose a plausible catalytic mechanism involving outer-sphere hydride delivery to the coordinated π-electrophile in conjunction with intramolecular, secondary-sphere boryl delivery from the assisting pyridonate ligand (Scheme 4C). These findings are consistent both with the observation of imine adduct **8** as the probable catalyst resting state and diboryl imine adduct **6** as an on-cycle intermediate. Additionally, the involvement of multiple units of HBpin in outer-sphere hydride delivery accounts for the strong sensitivity of the reaction yield to HBpin concentration. The absence of a discrete metal hydride intermediate accounts for the high chemoselectivity avoiding competitive chain-walking processes. Computational modeling at the ωB97XD/def2-TZVP/LANL2DZ(K) level of theory using acetonitrile as a model substrate enabled identification of several low-energy intermediates implicated in the outer-sphere hydride delivery mechanism (see Supporting Information). By contrast, intermediates on route to B–H oxidative addition and metal hydride formation were comparatively inaccessible energetically or could not be located as local stationary states.

As such, the computational and experimental findings provide substantial insight into the role of the pyridonate ligand in preorganizing the Lewis acidic boryl unit and Lewis basic nitrile in the secondary coordination sphere. We anticipate that these findings may prove general, enabling cooperative functionalization of a range of polar electrophiles.

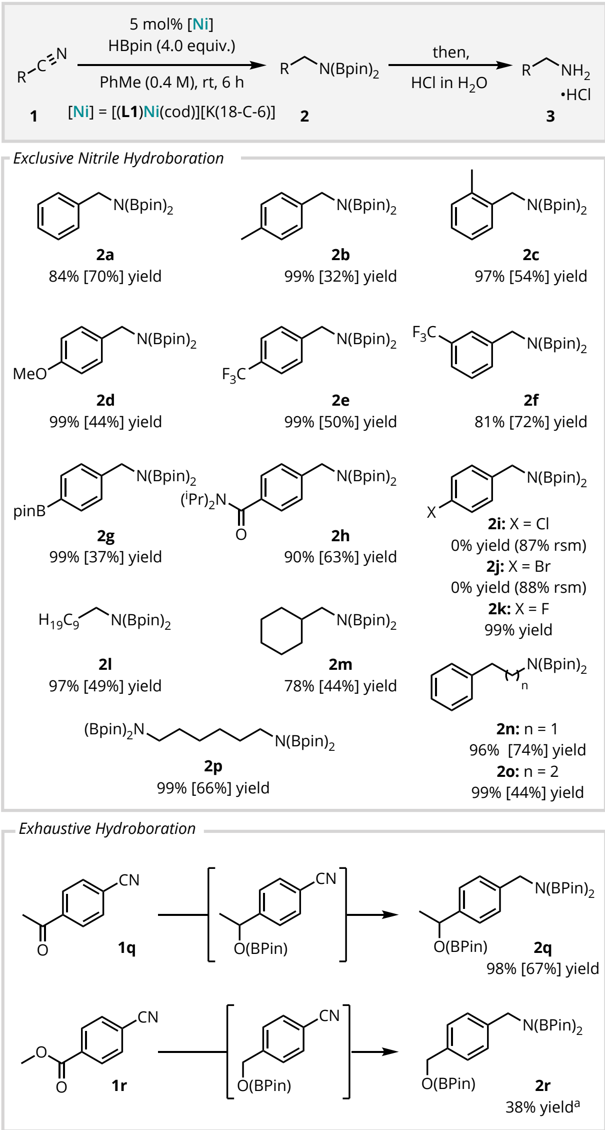

Scheme 3. Nitrile substrate scope. Reactions were conducted in duplicate using nitrile 1 (0.2 mmol, 1.0 equiv) and HBpin (4.0 equiv) with 5 mol% [K(18-crown-6)][(**L1**)Ni(cod)] (0.01 mmol) in PhMe (0.4 M) at room temperature for 6 h. Yields were determined from the relative ^{1}H NMR integration of **2** vs. 1,3,5-trimethoxybenzene (0.1 mmol) added after the reaction as an internal standard. Isolated yields of **3** are reported in brackets. [a] Mixture of hydroboration products.

Conflicts of interest

There are no conflicts to declare.

Acknowledgment

Financial support was provided by the University of Rochester and the David and Lucile Packard Foundation (#2022-74673). X.W. acknowledges the University of Rochester Discover Grant for a research fellowship. The NSF MRI program is acknowledged for the purchase of an X-ray diffractometer (CHE-1725028). The authors thank Ray Teng and Dr. Tessa Baker (University of Rochester) for technical assistance.

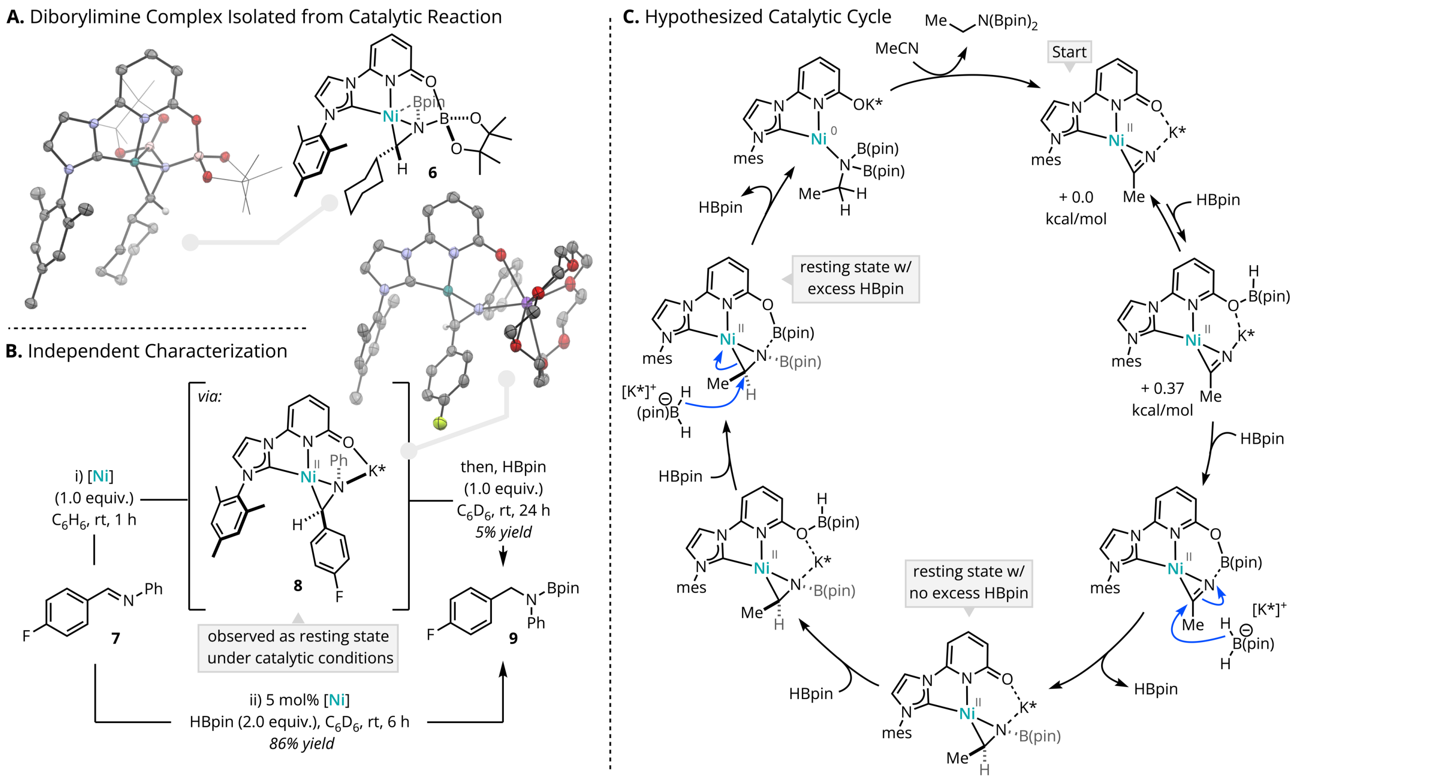

Scheme 4. Relevance of intermediate imine complexes suggesting a plausible mechanism for hydride and boryl delivery. Solid-state structures of **6** and **8** determined by SC-XRD. Thermal ellipsoids depicted at 50% probability. Most H atoms and co-crystallized solvent molecules omitted for clarity. Pinacol backbone represented as a wireframe for clarity. Reactions with substrate **7** performed in duplicates. Yield of **9** was determined from the relative ^{1}H NMR integration vs. 1,3,5-trimethoxybenzene (0.1 mmol) added after the reaction as an internal standard. Listed electronic energies (298 K) computed at the ωB97XD/def2-TZVP/SMD(MeCN) level of theory. See supporting information for additional details. [Ni] = [K(18-crown-6)][(**L1**)Ni(cod)]; K* = [K(18-crown-6)]$^{+}$. C = charcoal, N = blue, O = red, B = pink, F = yellow, Ni = teal.

Notes and references

1 K. Eller, E. Henkes, R. Rossbacher and H. Höke, in *Ullmann's Encyclopedia of Industrial Chemistry*, Wiley, 2000, DOI: 10.1002/14356007.a02_001.
2 P. Ertl, E. Altmann and J. M. McKenna, *J. Med. Chem.*, 2020, **63**, 8408–8418.
3 H.-U. Blaser and F. Spindler, in *Organic Reactions*, 2009, DOI: 10.1002/0471264180.or074.01, pp. 1-102.
4 T. Najam, S. S. A. Shah, K. Mehmood, A. U. Din, S. Rizwan, M. Ashfaq, S. Shaheen and A. Waseem, *Inorg Chim Acta*, 2018, **469**, 408–423.
5 H.-J. r. Arpe and K. Weissermel, *Industrial Organic Chemistry*, Wiley-VCH, Weinheim, Germany, 5th edn., 2010.
6 Y. Ding, X. Ma, Y. Liu, W. Liu, Z. Yang and H. W. Roesky, *Organometallics*, 2019, **38**, 3092–3097.
7 S. Das, S. L. Zhou, D. Addis, S. Enthaler, K. Junge and M. Beller, *Top Catal*, 2010, **53**, 979–984.
8 S. Werkmeister, K. Junge and M. Beller, *Org Process Res Dev*, 2014, **18**, 289–302.
9 T. Irrgang and R. Kempe, *Chem. Rev.*, 2020, **120**, 9583–9674.
10 A. R. Bazkiaei, M. Findlater and A. E. V. Gorden, *Org Biomol Chem*, 2022, **20**, 3675–3702.
11 M. R. Elsby and R. T. Baker, *Chem. Soc. Rev.*, 2020, **49**, 8933–8987.
12 C. Weetman, M. D. Anker, M. Arrowsmith, M. S. Hill, G. Kociok-Köhn, D. J. Liptrot and M. F. Mahon, *Chem. Sci.*, 2016, **7**, 628-641.
13 A. Harinath, J. Bhattacharjee and T. K. Panda, *Adv. Syn. Catal.*, 2019, **361**, 850-857.
14 B. Yan, X. He, C. Ni, Z. Yang and X. Ma, *Chem. Cat. Chem.*, 2021, **13**, 851–854.
15 F. Meger, A. C. W. Kwok, F. Gilch, D. R. Willcox, A. J. Hendy, K. Nicholson, A. D. Bage, T. Langer, T. A. Hunt and S. P. Thomas, *Beilstein J. Org. Chem.*, 2022, **18**, 1332–1337.
16 A. Y. Khalimon, P. Farha, L. G. Kuzmina and G. I. Nikonov, *Chem. Commun.*, 2012, **48**, 455-457.
17 J. B. Geri and N. K. Szymczak, *J. Am. Chem. Soc.*, 2015, **137**, 12808–12814.
18 A. D. Ibrahim, S. W. Entsminger and A. R. Fout, *Acs Catal*, 2017, **7**, 3730–3734.
19 G. Nakamura, Y. Nakajima, K. Matsumoto, V. Srinivas and S. Shimada, *Catal Sci Technol*, 2017, **7**, 3196–3199.
20 C. Ghosh, S. Kim, M. R. Mena, J.-H. Kim, R. Pal, C. L. Rock, T. L. Groy, M.-H. Baik and R. J. Trovitch, *J. Am. Chem. Soc.*, 2019, **141**, 15327-15337.
21 R. Thenarukandiyil, V. Satheesh, L. J. W. Shimon and G. de Ruiter, *Chem. Asian J.*, 2021, **16**, 999-1006.
22 M. R. Elsby, C. Oh, M. Son, S. Y. H. Kim, M.-H. Baik and R. T. Baker, *Chem. Sci.*, 2022, **13**, 12550–12559.
23 S. Ataie and R. T. Baker, *Inorg. Chem.*, 2022, **61**, 19998–20007.
24 B. J. H. Austen, M. L. Clapson and M. W. Drover, *RSC Adv.*, 2023, **13**, 19158–19163.
25 S. Ataie, J. S. Ovens and R. Tom Baker, *Chem. Commun.*, 2022, **58**, 8266-8269.
26 M. Afandiyeva, A. A. Kadam, X. J. Wu, W. W. Brennessel and C. R. Kennedy, *Organometallics*, 2022, **41**, 3014–3023.
27 A. D. Bage, T. A. Hunt and S. P. Thomas, *Org. Lett.*, 2020, **22**, 4107-4112.